Electronic Supplementary Material (ESI) for Inorganic Chemistry Frontiers.

Supplementary Information

One-Step CVD Fabrication and Optoelectronic Properties of SnS_2/SnS Vertical Heterostructures

Mingling Li,[a] Yunsong Zhu,[a] Taishen Li,[a] Yue Lin,[a] Hongbing Cai,[a] Sijia Li,[a] Huaiyi Ding,[a] Nan Pan[abc] and Xiaoping Wang*[abc]

[a]*Hefei National Laboratory for Physical Sciences at the Microscale and Department of Physics, University of Science and Technology of China, Hefei, Anhui 230026, P.R. China*
E-mail: xpwang@ustc.edu.cn

[b] *Synergetic Innovation Center of Quantum Information & Quantum Physics, University of Science and Technology of China, Hefei, Anhui 230026, P. R. China*

[c]*Key Laboratory of Strongly-Coupled Quantum Matter Physics, Chinese Academy of Sciences, School of Physical Sciences, University of Science and Technology of China, Hefei, Anhui 230026, P. R. China*

1. Characterizations of as-grown SnS flake.

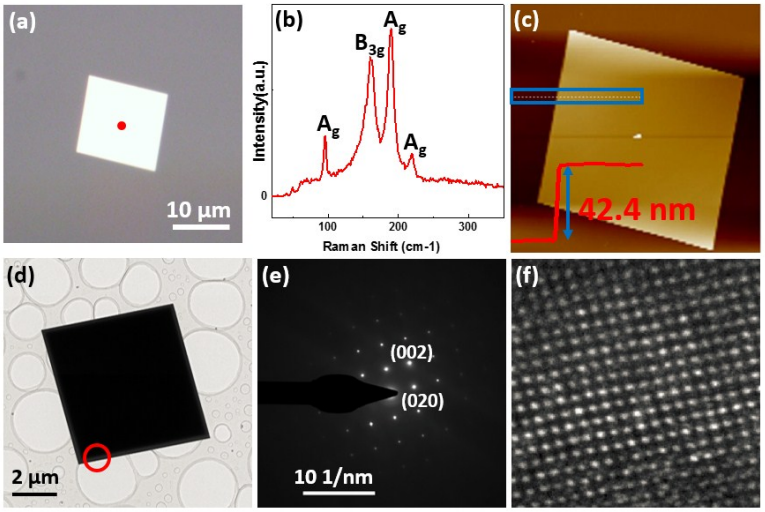

Fig. S1 Characterizations of the as-grown SnS flake. (a) Optical image, (b) Raman spectrum and (c) AFM image of the as-grown SnS flake. (d) TEM image, (e) SAED pattern and (f) HRTEM image of the as-grown SnS flake.

Fig. S1a shows optical image of an as-grown SnS flake, and Fig. S1b is the corresponding Raman spectrum, in which SnS Raman peaks located at 95.8 cm^{-1} (A_g), 161.2 cm^{-1} (B_{3g}), 189.5 cm^{-1}(A_g), 219.4 cm^{-1}(A_g) can be observed clearly. AFM characterization shown in Fig. S1c demonstrates

that the flake has smooth surface and the thickness is about 42 nm. Figs.S1d-1f are TEM image, corresponding SAED pattern and HRTEM image of the SnS flake, respectively. Clear lattice fringes can be found and the measured lattice constant along armchair (zigzag) direction is 4.38(4.02) Å, consistent with previous results, demonstrating the high quality of the SnS flake.

2. Characterizations of the as-grown pyramid-shaped SnS_2 flake

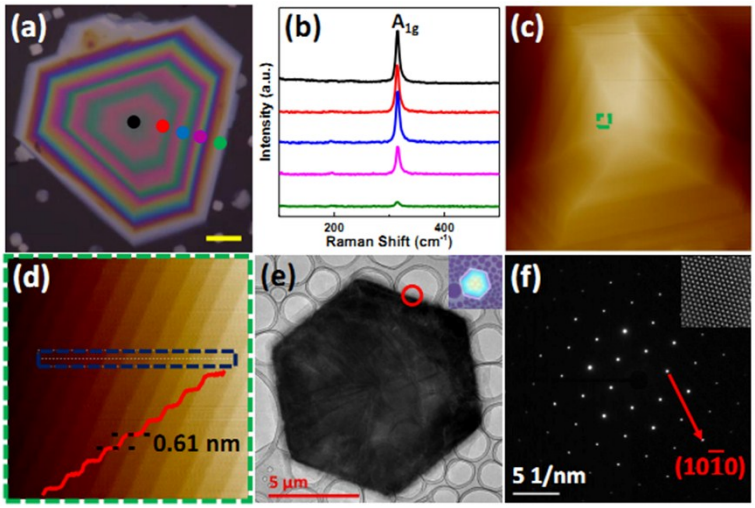

Fig. S2 Characterizations of the as-grown pyramid-shaped SnS_2 flake. (a) Optical photo and (b) Raman spectra of the SnS_2 flake taken at different positions shown in (a). (c) AFM and (d) enlarged AFM image of the SnS_2 flake. (e) Bright-field TEM image of the SnS_2 flake transferred on Cu mesh and inset is corresponding optical photo. (f) SAED pattern of the SnS_2 taken from the red circle in (e). Inset is corresponding HRTEM image.

As shown in Fig. S2a, the as-grown hexagonal flake with colorized stripes from edge to center is SnS_2, which can be identified by the corresponding Raman spectra of different positions all showing clear SnS_2 A_{1g} peak at 314 cm^{-1} in Fig. S2b. AFM image of Fig. S2c reveals the pyramid morphology of the SnS_2 flake. Fig. S2d demonstrates that the flake is constituted by SnS_2 monolayers with thickness of 0.61 nm. [1] To investigate the crystalline quality of SnS_2 flake, we transferred the pyramid-shaped SnS_2 flake onto a Cu mesh for TEM characterization, as shown in Fig. S2e. The sharp SAED spots in Fig. S2f with inset of clear HRTEM image verify the high quality of the as-grown pyramid-shaped SnS_2, and the interplanar distance of $(10\bar{1}0)$ is measured to be 3.18 Å, in accordance with previous result. [1]

3. EDX characterization of the SnS_2/SnS heterostructure and pyramid shaped SnS_2.

EDX characterization was first performed on the SnS_2/SnS heterostructure with different regions, as shown in Fig. S3. As seen, when the signal is selected from the region 01 (labeled with red box in the figure), the element ratio of S to Sn is about 1, indicating the composition of the region being SnS. As the probe moving to the region 02 (edge of the junction labeled with orange box) and region 03 (center of the junction labeled with cross mark), the ratio of S to Sn increases to

1.19 and 1.33, respectively. The result suggests that the SnS_2 component of the heterostructure increases from the edge to the center region, which is good agreement with the heterostructure morphology of pyramid-shaped SnS_2 on SnS flake. Additionally, EDX was also performed on the pure pyramid-shaped SnS_2 (Fig. S3f, 3g), and the result (Fig. S3h) demonstrates that the ratio of S to Sn is about 2, consistent with that of SnS_2.

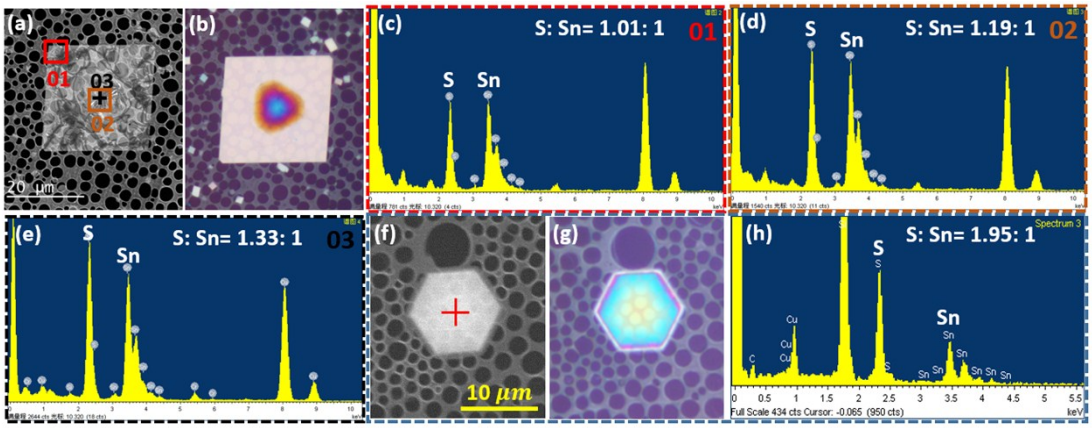

Fig. S3 EDX characterizations of the SnS_2/SnS heterostructure and pure SnS_2. (a) and (b) are TEM image and optical image of the SnS_2/SnS heterostructure, respectively. (c-e) The EDX spectra of the SnS area (red box), junction area (orange box) and center point (black cross) of the heterostructure, respectively. (f) and (g) are SEM image and optical image of the pyramid-shaped SnS_2 flake, respectively. (h) The EDX spectrum of the pure SnS_2 flake.

4. Raman mapping images of SnS_2/SnS heterostructure and SnS flake

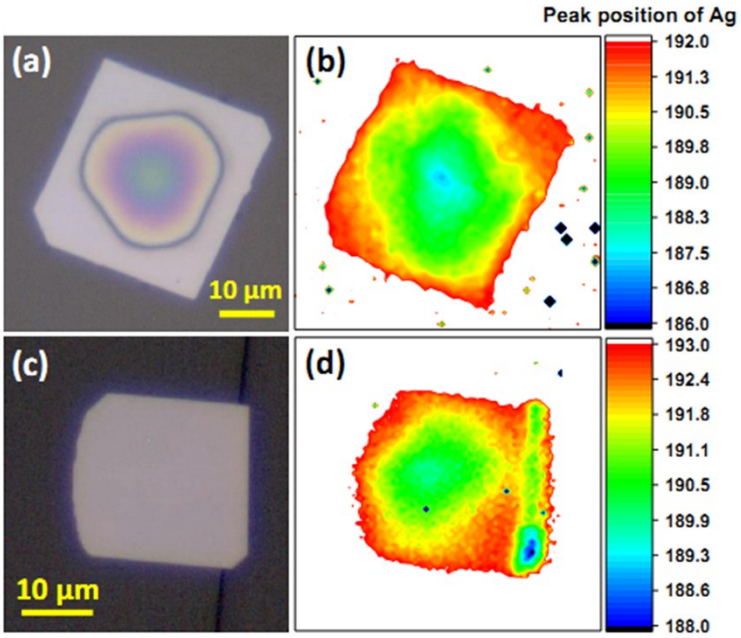

Fig. S4 (a) Optical photos of SnS_2/SnS heterostructure and (c) SnS flake. (b) Raman mapping images of SnS A_g 191.2 cm^{-1} mode from SnS_2/SnS heterostructure and (d) SnS flake.

Fig. S4a is the optical photos of SnS_2/SnS heterostructure, and Fig. S4b is the corresponding Raman mapping of SnS A_g (191.2 cm^{-1}) mode. As seen, the Raman peak red shift from edge to center, indicating there existed the tensile strain in the center of flake. The behavior is very similar to that observed from the as-grown single SnS flake (Fig. S4d), suggesting that the strain originates from the SnS flake growth.

5. Optical images of products with T3 at 410℃.

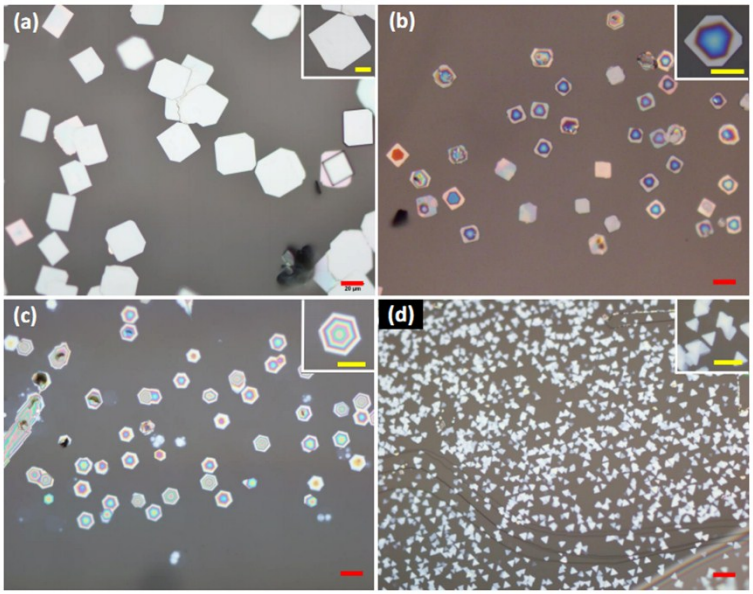

Fig. S5 (a)-(d) Optical images of the as-grown flakes on mica substrates placed at different positions. The insets are typically enlarged images of the corresponding flakes. The scale bars in the figures (insets) are 20 μm (10 μm).

Fig.S5 is the optical images of products when the temperature of T3 set to 410 ℃. It can be found that these products are very similar to those shown in Fig.1 in the main article, which were prepared with T3 ~450 ℃.

6. Observation of the deposition on quartz tube

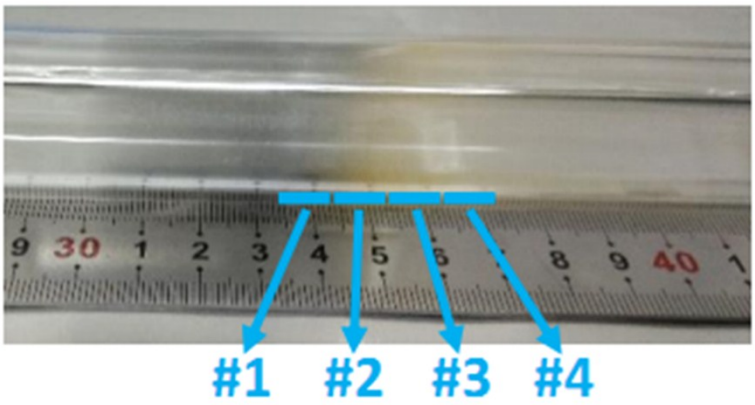

Fig. S6 Picture of a quartz tube around substrate area after one-step CVD growth.

Fig. S6 shows the quartz tube around substrate area after the one-step CVD growth. It can be found that the color on the wall of the quartz tube changes from grey to yellow from left to right. Because the colors of single crystals of SnS and SnS_2 are grey and yellow respectively,[2] the color variation on the tube indicates the product changes from SnS to SnS_2. This agrees well with our observation that SnS flakes formed on #1 substrate and SnS_2 flakes formed on #3 and #4 substrates, respectively. Moreover, as shown in Fig. S6, a great deal of SnS has been deposited on the wall of tube around the growth area, leading to the obvious decrease of the SnS vapor concentration along the transmit direction.

7. Characterizations of the conductive type of SnS_2 and SnS flakes

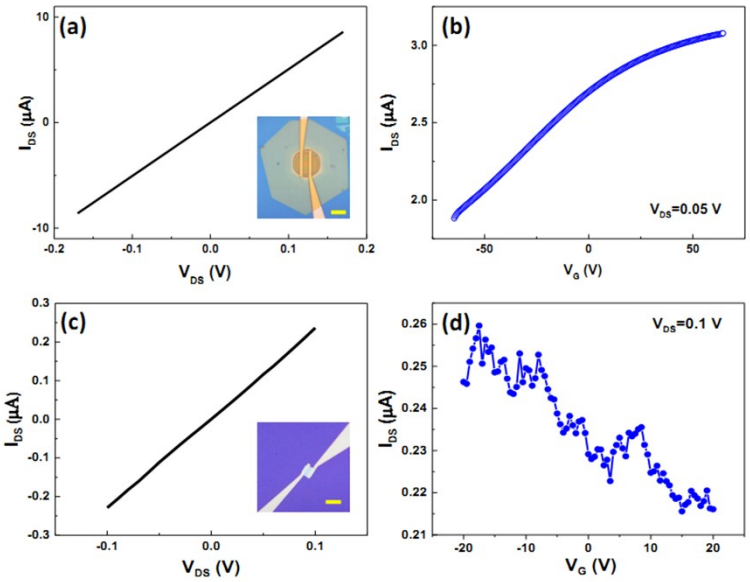

Fig. S7 (a) IV curve and (b) transfer curve of the as-grown SnS_2 flakes. Inset is the optical picture of the SnS_2 device. (c) IV curve and (d) transfer curve of the as-grown SnS flake. Inset is the optical picture of the SnS device. The scale bars of the insets are 10 μm.

To investigate the conductive type of the as-grown single SnS_2 and SnS flakes, [3] we fabricated the FET devices of the SnS_2 and SnS, respectively, as shown in the insets. The observed linear IV curves indicate the ohmic contacts of the devices. The transfer curves of the devices clearly demonstrate that the SnS_2 flake is n-type semiconductor while the SnS is p-type one. The carrier mobilities of single SnS_2 and SnS flakes estimated from the transfer characteristics are 5.3 $cm^2V^{-1}s^{-1}$ and 0.6 $cm^2V^{-1}s^{-1}$, respectively.

8. Carrier transport at the junction.

As shown in the Fig. S8, when the 660 nm laser illuminates on the sample, the photo-induced electron-hole pairs are formed in SnS. The electrons can be drifted to the SnS_2 region by the built in field near the junction and then diffused to the electrode, while the holes diffuse in the SnS and reach to the other electrode.

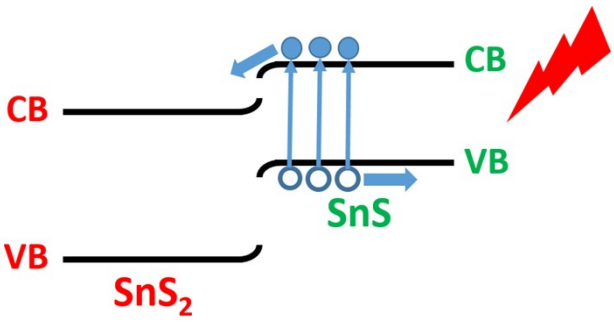

Fig. S8 The schematic graph of carrier transport at the junction.

9. Photoresponse of the heterostructure under 444 nm laser illumination.

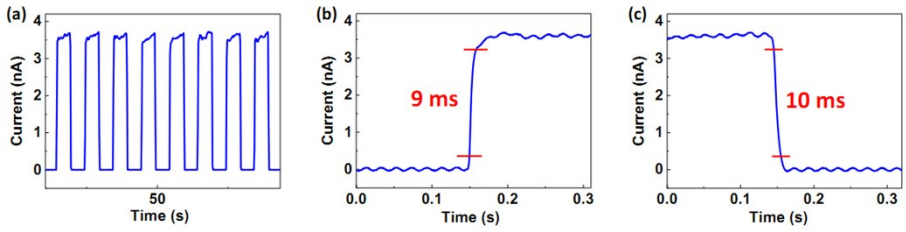

Fig. S9 (a) Time-resolved photoresponse of the device under 444 nm laser illumination with 384 mw/cm^2. (b) Rise and (c) decay curves of the device.

References

1. G. Su, V. G. Hadjiev, P. E. Loya, J. Zhang, S. Lei, S. Maharjan, P. Dong, M. A. P, J. Lou and H. Peng, *Nano Lett.*, 2015, **15**, 506-513.
2. L. A. Burton, D. Colombara, R. D. Abellon, F. C. Grozema, L. M. Peter, T. J. Savenije, G. Dennler and A. Walsh, *Chem. Mater.*, 2013, **25**, 4908-4916.
3. J. H. Ahn, M. J. Lee, H. Heo, J. H. Sung, K. Kim, H. Hwang and M. H. Jo, *Nano Lett.*, 2015, **15**, 3703-3708.